Journal of Engineering and Applied Sciences 14 (20): 7437-7441, 2019
ISSN: 1816-949X

Growth ZnO Nanorod Arrays and its Photocatalytic Activity Under Visible Light Irradiation

[1]Dinh Thi Thanh Tam, [2]Tran Thi Ngoc Quyen, [2]Thi Hanh Thu Vu and [1]Long Giang Bach
[1]NTT Institute of High Technology, Nguyen Tat Thanh University,
298-300A Nguyen Tat Thanh, Ho Chi Minh City, Vietnam
[2]Faculty of Physics and Engineering Physics, University of Science, VNU-HCM City,
227 Nguyen Van Cu, Ho Chi Minh City, Vietnam
blgiang@ntt.edu.vn

Abstract: In this study, visible light active Zinc Oxide Nanorod arrays (ZnO NRs) were successfully prepared by an electrochemical process using Al-doped ZnO film (AZO) as an electrode, followed by annealed in ambient at difference temperature (100-500°C). The as-prepared ZnO NRs were characterized by SEM, XRD and PL technique. From the XRD and SEM results, ZnO NRs possess hexagonal morphology with an average diameter of 50-60 nm and the average length of 1.2-1.3 μm was obtained. From PL spectrum, the annealed temperature significant effects on the surface defects in ZnO NRs which can be enhanced visible light absorption. Moreover, ZnO NRs sample annealed at 300°C exhibited the highest PL peak, having the highest formation rate of •OH radicals and the highest percentage of Methylene Blue (MB) removal (76.05%) under visible light irradiation. This result indicates that the formation rate of •OH radicals shows a good correlation with the photocatalytic activity.

Key words: ZnO nanorod arrays, photocatalysis, methylene blue, formation, hexagonal morphology, highest percentage

INTRODUCTION

Recently, semicondu738ctor photocatalysis techniques have been received much attention because they can completely degrade hazardous compounds in water, which can be mineralized to CO_2, H_2O and harmless inorganic anions (Alinsafi *et al*., 2007). Among many semiconductor nanomaterials, ZnO Nanorod arrays (ZnO NRs) with hexagonal wurtzite crystal has been a potential photocatalyst for photodegradation of organic pollutants due to its high electron mobility, chemical stability and large surface (Look, 2001). However, this material only shows photo response to UV irradiation due to its large band gap (E_g = 3.3 eV). UV irradiation is only 3-5% of solar light and thus, restrict their efficiently utilize solar energy. Various efforts to enhance photocatalytic activity of ZnO NRs have been studied. It has been shown that the absorption of ZnO NRs can is extended to the visible region of the solar spectra by metal or non-metal ion doping (Ullah and Dutta, 2008), turning of defects in ZnO NRs (Akir *et al*., 2016; Baruah *et al*., 2009; Sarkar *et al*., 2012) or the growth rate of nanostructures (Sathe *et al*., 2016). Among them an optimum defect by annealed in ambient is a most simple method. Defects in ZnO NRs include vacancies, interstitials or substitutions positions formation in the synthesis process. Those defects after optimum can create defect states between the valence band and the conduction band allows excitation of visible light to generate electron-hole pairs (Baruah *et al*., 2009; Kavitha *et al*., 2014).

In this study, we report the growth of ZnO Nanorod arrays (ZnO NRs) on Aluminum-doped ZnO (AZO) thin film and their activity for the photodecomposition of Methylene Blue (MB) under UV and solar light irradiation. We, also investigated the effect of annealed temperature on defects in ZnO NRs.

MATERIALS AND METHODS

Synthesis and Characterizations: ZnO NRs/AZO/ITO was synthesized by coupling an electrochemical deposition method and calcination method. Firstly, AZO thin film with 200 nm thickness and 65 Ω^2 was deposited on top ITO substrate by DC magnetron sputtering

Corresponding Author: Long Giang Bach, NTT Institute of High Technology, Nguyen Tat Thanh University, 298-300A Nguyen Tat Thanh, Ho Chi Minh City, Vietnam, blgiang@ntt.edu.vn

system using Al_2O_3 2 wt.%-doped ZnO target. The electrodeposition was carried out potentiostatically at an applied power of 56 W and Ar pressure of 3×10^{-3} Torr, the fixed space between the target and substrate was 7 cm. Then, the ZnO NRs prepared on AZO film through electrochemical deposition method (Voltage 2.4 V and current 1 mA). Precursor solution containing Zn $(NO_3)_2$ (5.0 mM) and $C_6H_{12}N_4$ (5.0 mM) was stirred at 85°C for 30 min before growing process. AZO thin film and a platinum wire served as the cathode and the anode, respectively. In addition, AZO thin film also set as seeding layers, so, ZnO NRs could grow up directly on it. Finally, the samples were rinsed with deionized water to remove precursor and annealed at several temperatures 100-500°C for 1 h.

The morphology and size were observation by scanning electron microscopy (SEM, Hitachi S-4800). The X-Ray Diffraction (XRD) patterns were performed using a Bruker D8 ADVANCE X-ray diffractometer. Photoluminescence (PL) spectra were collected on a Horiba iHR320 spectrometer using a xenon lamp as the excitation source at room temperature.

Photocatalytic test: The photocatalytic performances of ZnO NRs were studied by the photocatalytic degradation MB under visible light irradiation using a 300 W solar lamp Ultra Vitalux (Osram) and Ultraviolet light (UV) using an 8 W UV lamp. In the typical reaction, the sample was immersed in 10 mL MB solution (5 ppm). Prior irradiation, the mixture was vigorously, stirred in the dark for 30 min to ensure adsorption-desorption equilibrium between the catalyst surface and MB molecules. About 3 mL of suspension was withdrawn at 15 min intervals for testing adsorption. The decrease in the MB concentration was measured on a UV-Vis spectrophotometer by recording the variations of the absorption band at 664 nm.

The formation of hydroxyl radicals (˙OH): The formation of hydroxyl radicals (˙OH) in the ZnO NRs/AZO system was detected by the fluorescence technique using Terephthalic Acid (TPA) as a probe molecule. When ˙OH radical generated from the visible light illuminated catalyst surfaces reacts with TPA, 2-Hydroxyterephthalic Acid (HTA) with a strong fluorescence characteristic at 425 nm peak was produced. The PL peak intensity of HTA is in proportion to the amount of ˙OH radicals produced in water. The experiment processes were the same processes as the measurement of the photocatalytic test by replacing the aqueous solution of MB with the aqueous solution of TPA (10 mL, TPA = 0.5 mM and NaOH = 2 mM). Fluorescence spectra were recorded on a Horiba iHR320 fluorescence spectrophotometer.

RESULTS AND DISCUSSION

Characterization and defects of ZnO NRs: The morphologies of ZnO NRs as grown were firstly studied by SEM technique as shown in Fig. 1a, b. From Fig. 1a, b, ZnO NRs possess morphology of hexagonal with an average diameter of 50-60 nm and the average length of 1.2-1.3 μm; the crystals showed high-density uniform and the vertical orientation on top the substrate. The XRD pattern (Fig. 1c) confirmed that the ZnO NRs have the hexagonal wurtzite crystal structure. The strong shape peak at $2\theta = 34.5°$ indicated the preferential orientation of the ZnO NRs along the (002) crystal plane. This suggests that ZnO NRs have a good crystal and c-direction.

The effects of annealing temperatures on surface defects in ZnO NRs were characterized by Photoluminescence (PL) (Fig. 1d). The luminescence of ZnO NRs includes two peaks. The UV peak at 380 nm corresponding to the violet emission, the main source of this emission is due to the band to band of ZnO. However, ZnO band gap with 3.3 eV is respected to 365 nm of violet emission. This position change can be explained due to the influence by ZnO excitation energy as large as 60 meV and defect of Zinc interstitial (Z_{ni}) energy level was found at 0.22 eV under the conduction band (Alvi *et al*., 2011). Another peak broad at 500-700 nm was reported emission from the surface defects. The common defects in ZnO NRs structure consist of oxygen Vacancies (V_O), zinc Vacancies (V_{Zn}), Oxygen interstitial (O_i) and Zinc interstitial (Z_{ni}). These peak bands are created by components of three shifts, recombination of hole and electron at oxygen Vacancies V_{O++} at 585 nm, recombination of holes and electron at V_{O+} green emission at 530 nm, chemical adsorption or desorption of oxygen, or H_2O corresponding to orange-red shift 640-650 nm (Van Dijken *et al*., 2000; Hofmann *et al*., 2007; Tang *et al*., 2015) Fig. 1d indicated that when increasing the annealed temperature from 100-500°C, the relative intensity of UV peak increased due to the completion of the ZnO NRs structure. In addition, we also observed that with a lower annealed temperature (<300°C), the relative intensity of visible peak (500-700 nm) increased, leading to the formation of increase surface defects density. This source may contribute to geometrical characteristics of hexagonal wurtzite crystalline structure.

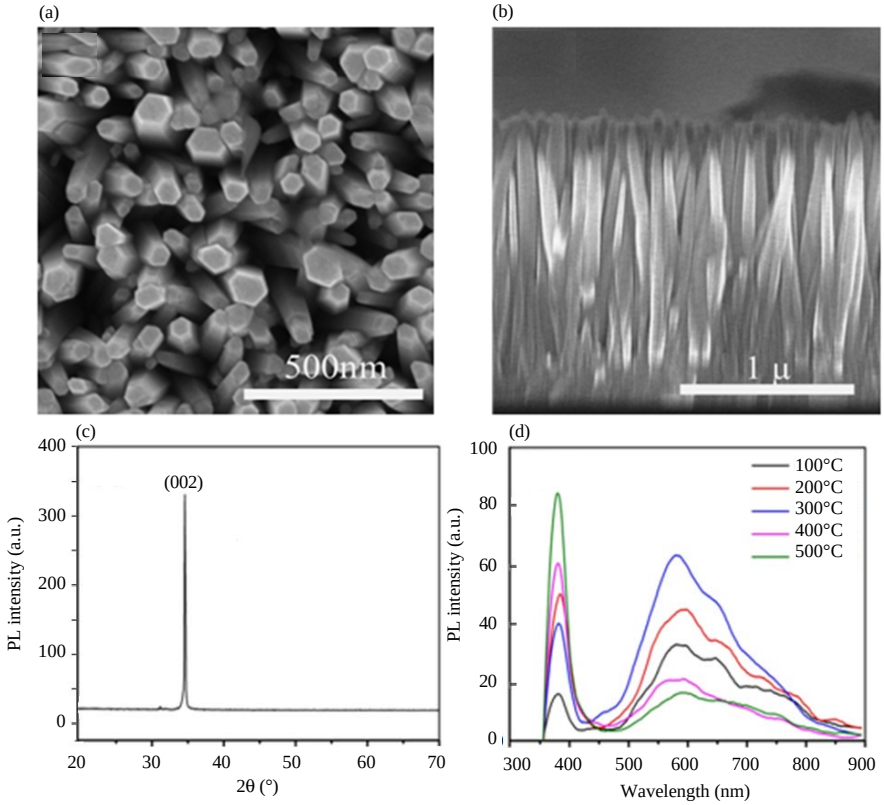

Fig. 1: a, b) SEM of ZnO NRs as grown on AZO electrodes using electrochemical deposition; c) XRD pattern of ZnO NRs as grown and d) Photoluminescence (PL) spectra of the ZnO NRs at several temperatures, 100- 500°C obtained with excitation wavelength of 325 nm

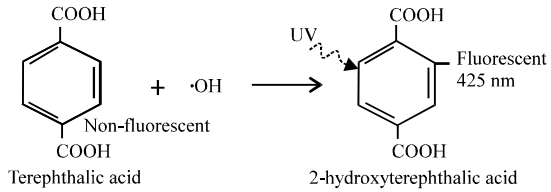

Fig. 2: Formation of 2-hydroxyterephthalic acid due to the reaction between terephthalic acid and hydroxyl radical of ZnO NRs under visible light irradiation

The wurtzite hexagonal crystalline structure of ZnO NRs has the value for hexagonal cell c/a = 1.606, the c axis being prioritized and the vertical (c-axis) energy required for crystal growth is small. So, diffusion of defects in structure will prioritize to this direction. When annealed temperature increases, Zn-O bonding can be enhanced, so, the defects in structure, if ZnO NRs will move to the surface. In this case, the increase of annealed temperatures from 100-300°C may conducive to the removal of oxygen vacancy defects to the surface, corresponding to the increase of intensity emission at 530-585 nm. However, when the annealed temperature was increased to 400-500°C, these defects at the surface were filled with oxygen in the air to complete the ZnO structure for that reason reduction emission intensity at this peak. The remarkably close correlation of annealed temperature on the surface defects in ZnO NRs which can be improved the visible light absorption.

The formation of hydroxyl radicals (˙OH) and visible photocatalytic degradation of MB: Figure 3c shows the changes of PL spectra of TPA solution after 120 min exposed under visible light irradiation on ZnO NRs samples. HTA with a strong fluorescence characteristic at 425 nm peak obtained by the reaction of TA with the ˙OH radical formed on the interface of the photocatalyst water during irradiation (Fig. 2).

As shown in Fig. 3c, a blue emission signal at approximately 425 nm was observed in the presence of a catalyst. ZnO NRs sample annealed at 300°C showed the highest intensity among all samples. As mention above, the PL peak intensity of HTA is in proportion to the formation rate of ˙OH radicals produced in water which shows a good correlation with the photocatalytic activity.

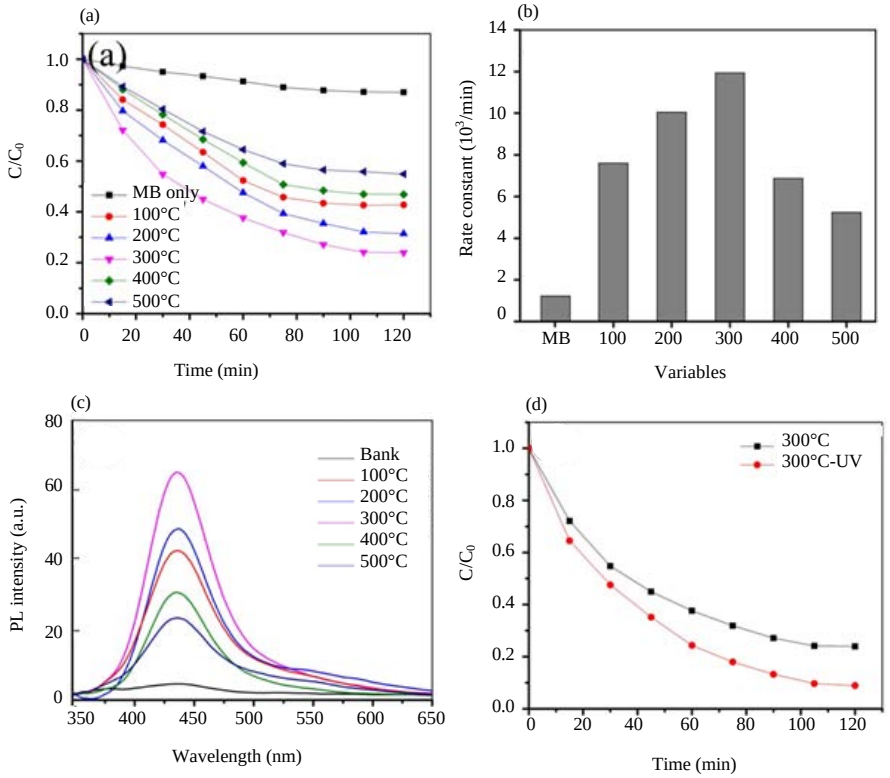

Fig. 3: a) Photocatalytic degradation chart of Methylene Blue (MB) solution under visible light irradiation with ZnO NRs photocatalysts annealed at different temperatures (100-500°C for 120 min); b) Degradation kinetics of MB; c) Photoluminescence (PL) spectra of terephthalic acid solution after 90 min exposed in visible light with ZnO NRs immersed and d) Photocatalytic degradation chart of Methylene Blue (MB) solution under UV and visible light irradiation with ZnO NRs photocatalysts annealed at 300°C for 120 min

As shown in Fig 3a, ZnO NRs annealed at 300°C exhibited highest, about 76.05% of MB was decomposed after 120 min light on. The removal fraction of MB is about 68.58 and 57.27% for systems with the samples annealed at 200 and 100°C, respectively. The samples annealed at temperature 400 and 500°C exhibited a decrease photocatalytic activities for MB degradation, accounting for 53.17 and 45.15%, respectively. The rate constants MB photocatalytic degradation with differently annealed ZnO NRs in Fig. 3b shows when increasing annealing temperatures up to 300°C, the MB degradation rate constants was increased. While annealing temperatures higher than 300°C, the degradation was reduced. This result correlated with visible light photocatalytic activity and surface defect states on ZnO NRs. Sub-bandgap formed from the surface that allows the transitions and generating active e-h pairs under visible light irradiation and thus, improve optical absorption (Al-Sabahi *et al*., 2016; Kavitha *et al*., 2014). However, when ZnO NRs were annealed at temperatures higher than 300°C, the degradation rate constant was found increase. These results also support that can be optimum surface defects in ZnO NRs to enhance efficiency photocatalytic in visible light.

ZnO NRs annealed at 300°C were exposed to visible light and UV light for comparison (Fig. 3d). Results after 120 min exposed degradation of 91.08% MB under UV light and degradation 76.05% under visible light. This result shows the potential for photocatalytic application under the sunlight (including both UV and visible light) of this material after annealed with high efficiency.

CONCLUSION

We successfully, prepared ZnO NRs by an electrochemical process using Al-doped ZnO film (AZO) as an electrode. As the results, the annealed temperature significant effects on the surface defects in ZnO NRs. ZnO NRs sample annealed at 300°C exhibited the highest PL peak, having the highest formation rate of •OH radicals and showed excellent catalytic activity for the decomposition MB.

ACKNOWLEDGEMENT

This research is funded by NTTU Foundation for Science and Technology Development under grant number 2017.01.15/HĐ-KHCN.

REFERENCES

Akir, S., A. Barras, Y. Coffinier, M. Bououdina and R. Boukherroub *et al*., 2016. Eco-friendly synthesis of ZnO nanoparticles with different morphologies and their visible light photocatalytic performance for the degradation of Rhodamine B. Ceram. Intl., 42: 10259-10265.

Al-Sabahi, J., T. Bora, M. Al-Abri and J. Dutta, 2016. Controlled defects of Zinc oxide nanorods for efficient visible light photocatalytic degradation of phenol. Mater., 9: 1-10.

Alinsafi, A., F. Evenou, E.M. Abdulkarim, M.N. Pons and O. Zahraa *et al*., 2007. Treatment of textile industry wastewater by supported photocatalysis. Dyes Pigm., 74: 439-445.

Alvi, N.H., K. Ul Hasan, O. Nur and M. Willander, 2011. The origin of the red emission in n-ZnO nanotubes/p-GaN white light emitting diodes. Nanoscale Res. Lett., 6: 1-7.

Baruah, S., S.S. Sinha, B. Ghosh, S.K. Pal and A.K. Raychaudhuri *et al*., 2009. Photoreactivity of ZnO nanoparticles in visible light: Effect of surface states on electron transfer reaction. J. Appl. Phys., 105: 074308-074308.

Hofmann, D.M., D. Pfisterer, J. Sann, B.K. Meyer and R. Tena-Zaera *et al*., 2007. Properties of the oxygen vacancy in ZnO. Appl. Phys. A, 88: 147-151.

Kavitha, M.K., K.B. Jinesh, R. Philip, P. Gopinath and H. John, 2014. Defect engineering in ZnO nanocones for visible photoconductivity and nonlinear absorption. Phys. Chem. Chem. Phys., 16: 25093-25100.

Look, D.C., 2001. Recent advances in ZnO materials and devices. Mater. Sci. Eng., B80: 383-387.

Sarkar, S., A. Makhal, T. Bora, K. Lakhsman and A. Singha *et al*., 2012. Hematoporphyrin-ZnO nanohybrids: Twin applications in efficient visible-light photocatalysis and dye-sensitized solar cells. ACS. Appl. Mater. Interf., 4: 7027-7035.

Sathe, P., M.T.Z. Myint, S. Dobretsov and J. Dutta, 2016. Removal and regrowth inhibition of microalgae using visible light photocatalysis with ZnO nanorods: A green technology. Sep. Purif. Technol., 162: 61-67.

Tang, Y., H. Zhou, K. Zhang, J. Ding and T. Fan *et al*., 2015. Visible-light-active ZnO via. oxygen vacancy manipulation for efficient formaldehyde photodegradation. Chem. Eng. J., 262: 260-267.

Ullah, R. and J. Dutta, 2008. Photocatalytic degradation of organic dyes with manganese-doped ZnO nanoparticles. J. Hazard. Mater., 156: 194-200.

Van Dijken, A., E.A. Meulenkamp, D. Vanmaekelbergh and A. Meijerink, 2000. Identification of the transition responsible for the visible emission in ZnO using quantum size effects. J. Lumin., 90: 123-128.